2019

Growth Kinetics, Carbon Isotope Fractionation, and Gene Expression in the Hyperthermophile Methanocaldococcus jannaschii during Hydrogen-Limited Growth and Interspecies Hydrogen Transfer

Begüm D. Topçuoğlu
University of Massachusetts Amherst

Cem Meydan
Weill Cornell Medical College

Tran B. Nguyen
University of South Carolina - Columbia

Susan Q. Lang
University of South Carolina - Columbia

James F. Holden
University of Massachusetts Amherst, jholden@microbio.umass.edu

Recommended Citation

Topçuoğlu, Begüm D.; Meydan, Cem; Nguyen, Tran B.; Lang, Susan Q.; and Holden, James F., "Growth Kinetics, Carbon Isotope Fractionation, and Gene Expression in the Hyperthermophile Methanocaldococcus jannaschii during Hydrogen-Limited Growth and Interspecies Hydrogen Transfer" (2019). *Applied and Environmental Microbiology*. 321.
http://dx.doi.org/10.1128/AEM.00180-19

AMERICAN SOCIETY FOR MICROBIOLOGY | Applied and Environmental Microbiology®

GEOMICROBIOLOGY

Growth Kinetics, Carbon Isotope Fractionation, and Gene Expression in the Hyperthermophile *Methanocaldococcus jannaschii* during Hydrogen-Limited Growth and Interspecies Hydrogen Transfer

Begüm D. Topçuoğlu,[a]* Cem Meydan,[b] Tran B. Nguyen,[c] Susan Q. Lang,[c] James F. Holden[a]

[a]Department of Microbiology, University of Massachusetts, Amherst, Massachusetts, USA
[b]Institute for Computational Biomedicine, Weill Cornell Medical College, New York, New York, USA
[c]School of the Earth, Ocean, and Environment, University of South Carolina, Columbia, South Carolina, USA

ABSTRACT Hyperthermophilic methanogens are often H_2 limited in hot subseafloor environments, and their survival may be due in part to physiological adaptations to low H_2 conditions and interspecies H_2 transfer. The hyperthermophilic methanogen *Methanocaldococcus jannaschii* was grown in monoculture at high (80 to 83 μM) and low (15 to 27 μM) aqueous H_2 concentrations and in coculture with the hyperthermophilic H_2 producer *Thermococcus paralvinellae*. The purpose was to measure changes in growth and CH_4 production kinetics, CH_4 fractionation, and gene expression in *M. jannaschii* with changes in H_2 flux. Growth and cell-specific CH_4 production rates of *M. jannaschii* decreased with decreasing H_2 availability and decreased further in coculture. However, cell yield (cells produced per mole of CH_4 produced) increased 6-fold when *M. jannaschii* was grown in coculture rather than monoculture. Relative to high H_2 concentrations, isotopic fractionation of CO_2 to CH_4 ($\varepsilon_{CO2\text{-}CH4}$) was 16‰ larger for cultures grown at low H_2 concentrations and 45‰ and 56‰ larger for *M. jannaschii* growth in coculture on maltose and formate, respectively. Gene expression analyses showed H_2-dependent methylene-tetrahydromethanopterin (H_4MPT) dehydrogenase expression decreased and coenzyme F_{420}-dependent methylene-H_4MPT dehydrogenase expression increased with decreasing H_2 availability and in coculture growth. In coculture, gene expression decreased for membrane-bound ATP synthase and hydrogenase. The results suggest that H_2 availability significantly affects the CH_4 and biomass production and CH_4 fractionation by hyperthermophilic methanogens in their native habitats.

IMPORTANCE Hyperthermophilic methanogens and H_2-producing heterotrophs are collocated in high-temperature subseafloor environments, such as petroleum reservoirs, mid-ocean ridge flanks, and hydrothermal vents. Abiotic flux of H_2 can be very low in these environments, and there is a gap in our knowledge about the origin of CH_4 in these habitats. In the hyperthermophile *Methanocaldococcus jannaschii*, growth yields increased as H_2 flux, growth rates, and CH_4 production rates decreased. The same trend was observed increasingly with interspecies H_2 transfer between *M. jannaschii* and the hyperthermophilic H_2 producer *Thermococcus paralvinellae*. With decreasing H_2 availability, isotopic fractionation of carbon during methanogenesis increased, resulting in isotopically more negative CH_4 with a concomitant decrease in H_2-dependent methylene-tetrahydromethanopterin dehydrogenase gene expression and increase in F_{420}-dependent methylene-tetrahydromethanopterin dehydrogenase gene expression. The significance of our research is in understanding the nature of hyperthermophilic interspecies H_2 transfer and identifying biogeochemical and molecular markers

Citation Topçuoğlu BD, Meydan C, Nguyen TB, Lang SQ, Holden JF. 2019. Growth kinetics, carbon isotope fractionation, and gene expression in the hyperthermophile *Methanocaldococcus jannaschii* during hydrogen-limited growth and interspecies hydrogen transfer. Appl Environ Microbiol 85:e00180-19. https://doi.org/10.1128/AEM.00180-19.

Editor Robert M. Kelly, North Carolina State University

Address correspondence to James F. Holden, jholden@microbio.umass.edu.

* Present address: Begüm D. Topçuoğlu, Department of Microbiology & Immunology, University of Michigan, Ann Arbor, Michigan, USA.

This article is C-DEBI contribution number 465.

Received 21 January 2019
Accepted 15 February 2019
Accepted manuscript posted online 1 March 2019
Published 18 April 2019

for assessing the physiological state of methanogens and possible source of CH_4 in natural environments.

KEYWORDS *Methanocaldococcus*, RNA-Seq, *Thermococcus*, carbon isotope fractionation, hydrogen, hyperthermophiles, methanogenesis, syntrophs

Each year, approximately 1 Pg of CH_4 is produced globally through methanogenesis, largely by methanogens growing syntrophically with fermentative microbes that hydrolyze biopolymers (1), but little is known about the magnitude or mechanism of methanogenesis through thermophilic H_2 syntrophy or interspecies H_2 transfer. Deep-sea hydrothermal vents are known habitats for thermophilic methanogens (2). It was also estimated that 35% of all marine sediments are above 60°C (3), suggesting that these environments likewise provide a large global biotope for thermophiles. Microcosms containing low-temperature hydrothermal fluid as well as an archaeal coculture derived from a high-temperature oil pipeline each produced CH_4 through interspecies H_2 transfer at 80°C when supplemented with organic compounds, both without added H_2 (4, 5). Both showed that CH_4 was produced from a mixed microbial community consisting of the hyperthermophilic H_2-producing heterotroph *Thermococcus* and the (hyper)thermophilic, hydrogenotrophic methanogens *Methanocaldococcus*, *Methanothermococcus*, and *Methanothermobacter*.

Molecular and culture-dependent analyses show that *Thermococcus* and thermophilic methanogens are collocated in hydrothermal vents (5–11), waters produced by high-temperature petroleum reservoirs (12–19), and mid-ocean ridge flanks (20). In high-temperature, organic-rich environments, such as petroleum reservoirs, collocated H_2-producing heterotrophs are the primary source of H_2 (21), but very little is known about this process at high temperatures or how thermophilic syntrophy affects environmental signals.

In this study, growth and CH_4 production kinetics, carbon isotope fractionation, and gene expression data were examined together for a hyperthermophilic methanogen under conditions ranging from monoculture growth at high and low H_2 concentrations to coculture growth with an H_2-producing partner. The hyperthermophile *Methanocaldococcus jannaschii* was grown in monoculture in a chemostat under H_2-replete and H_2-limited conditions based on previous kinetic experiments (9). It was also grown with the H_2-producing hyperthermophilic heterotroph *Thermococcus paralvinellae* using maltose and formate separately as the growth substrates (22). The purpose was to determine if *M. jannaschii* cell yield (amount of biomass produced per mole of CH_4 produced, or Y_{CH4}) increases when cultures are shifted from H_2-replete to H_2-limited growth conditions and if Y_{CH4} remains high or increases further during interspecies H_2 transfer. This study also examined if interspecies H_2 transfer stimulates the growth rate or cell yield of *T. paralvinellae* or ameliorates its H_2 inhibition relative to its growth in monoculture. Furthermore, isotopic carbon fractionation was examined to determine if CH_4 is isotopically lighter when H_2 flux is reduced, as previously observed in moderately thermophilic methanogens (23–25). Finally, differential gene expression analysis using transcriptome sequencing (RNA-Seq) was used to determine if changes occur in *M. jannaschii* for the expression of genes for carbon assimilation, CH_4 production, or energy generation when H_2 decreases in availability. This study demonstrates the utility of measuring growth kinetic parameters, carbon isotope fractionation, and differential gene expression patterns for two species grown in coculture. The data elucidate how hyperthermophilic methanogens behave in a high H_2 flux environment, such as those found at some hydrothermal vents, versus a low H_2 flux environment, such as petroleum reservoirs.

RESULTS

Growth parameters for mono- and cocultures. A summary of the growth conditions is provided in Table 1. In monoculture, the specific growth rate of *M. jannaschii* in the chemostat decreased from 1.04 ± 0.12 h^{-1} (± standard errors) when grown on 80

TABLE 1 Carbon isotopic composition of CO_2 and CH_4 of culture and coculture experiments

Growth condition	Initial H_2 (aq[c]) (μM)	$\delta^{13}C$ value (‰)			
		CO_2 (aq)			
		T_o	T_f	CH_4, T_f	$\varepsilon_{CO2\text{-}CH4}$ (‰)
M. jannaschii only					
Chemostat R1	83	−35.1	−29.0	−55.9	28.5
Chemostat R2	80	−34.6	−28.2	−55.9	29.3
Chemostat R3	80	−35.2	−28.4	−55.8	29.0
Chemostat R4	18	−35.9	−33.3	−75.7	45.9
Chemostat R5	15	−35.7	−31.8	−74.2	45.8
Chemostat R6	27	−35.8	−32.0	−72.5	43.7
Bottle B1	1,200[a]	−26.1	+22.6	−32.9	22.1[b]
Bottle B2	1,200[a]	−26.1	+19.2	−34.2	23.0[b]
M. jannaschii-T. paralvinellae coculture					
Bottle B3 (formate)	0	−26.7	−22.8	−99.4	85.1
Bottle B4 (formate)	0	−26.7	−23.0	−99.4	84.8
Bottle B5 (maltose)	0	−25.5	−24.4	−91.2	73.5
Bottle B6 (maltose)	0	−25.5	−21.6	−89.0	73.9

[a]Estimated at 82°C using the Geochemist's Workbench Standard 10.0 (Aqueous Solutions, LLC, Champaign, Illinois, USA).
[b]Calculated based on the isotopic compositions of the starting CO_2, final CO_2, and accumulated methane.
[c]aq, aqueous concentration.

to 83 μM H_2 to 0.50 ± 0.09 h^{-1} when grown on 15 to 27 μM H_2 (Fig. 1A). Cell concentrations in the medium and H_2 and CH_4 concentrations in the headspace remained constant throughout growth in the chemostat (see Fig. S1 in the supplemental material). Attempts to grow *M. jannaschii* in coculture with *T. paralvinellae* in the chemostat when either maltose or formate was the energy source, with and without stirring and gas sparging of the medium with CO_2 and N_2, were unsuccessful. This was likely due to the open reactor that permits gas to flow out of the reactor without any gas pressure increase. Coculture growth was readily established in sealed bottles that contained 1 atm of gas pressure at room temperature. At 82°C, the gas pressure in the bottle was 1.2 atm, which slowed H_2 efflux from the growth medium to the headspace. Therefore, the cocultures were grown in sealed bottles with the same volume of medium and headspace as the chemostat. The growth rates of *M. jannaschii* decreased further when it was grown in coculture with *T. paralvinellae* to 0.12 ± 0.01 h^{-1} and 0.22 ± 0.03 h^{-1} when *T. paralvinellae* was grown on maltose and formate, respectively (Fig. 1A). Relative to H_2 concentrations when *T. paralvinellae* was grown in the bottles in monoculture, nearly all the H_2 was removed from the coculture bottles and CH_4 was produced (Fig. S2).

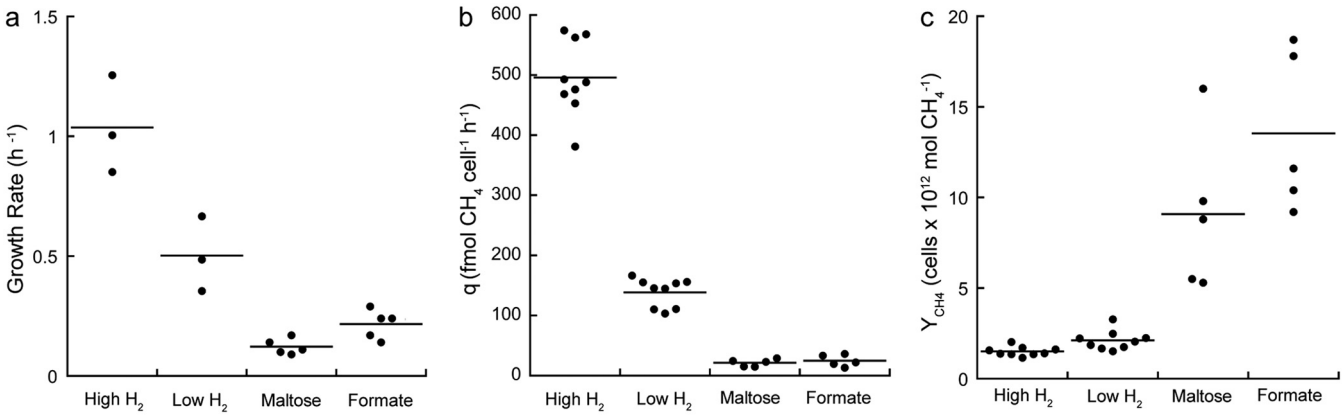

FIG 1 (a to c) Specific growth rate (a), cell-specific CH_4 production rate (q) (b), and cell yield (Y_{CH4}) (c) for *M. jannaschii* grown in monoculture in the chemostat with high (80 to 83 μM) and low (15 to 27 μM) aqueous H_2 concentration and grown in coculture with *T. paralvinellae* in bottles using maltose and formate as growth substrates. The horizontal bar represents the mean value.

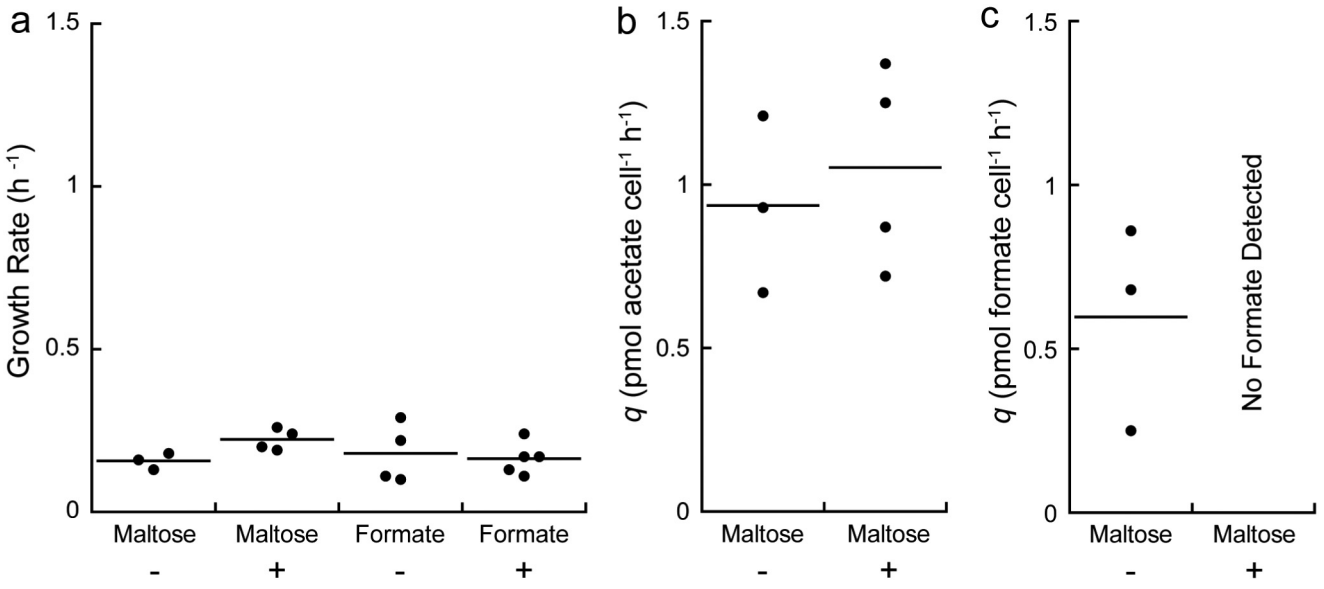

FIG 2 (a) Specific growth rate for *T. paralvinellae* grown in bottles in monoculture (−) and in coculture with *M. jannaschii* (+) on either maltose or formate. (b and c) Cell-specific production rate for acetate (b) and formate (c) for *T. paralvinellae* grown on maltose in monoculture (−) and in coculture with *M. jannaschii* (+). The horizontal bar represents the mean value.

The cell-specific CH_4 production rate decreased 3.6-fold when *M. jannaschii* was grown on 15 to 27 μM H_2 (139 ± 8 fmol cell^{-1} h^{-1}) relative to growth on 80 to 83 μM H_2 (496 ± 21 fmol cell^{-1} h^{-1}) (Fig. 1B). The rates decreased further when grown in coculture on maltose (21.3 ± 2.7 fmol cell^{-1} h^{-1}) and on formate (24.8 ± 4.3 fmol cell^{-1} h^{-1}) (Fig. 1B). However, the growth yields (Y_{CH4}) for *M. jannaschii* grown in coculture were significantly higher when grown on maltose (9.1 ± 1.9 [×10^{12}] cells per mol CH_4) and formate (13.5 ± 2.0 [×10^{12}] cells per mol CH_4) than growth yields in monoculture on 15 to 27 μM H_2 (2.1 ± 0.2 [×10^{12}] cells per mol CH_4) and 80 to 83 μM H_2 (1.5 ± 0.1 [×10^{12}] cells per mol CH_4) (Fig. 1C). Summaries of the growth and CH_4 production kinetics data for *M. jannaschii* are available in the supplemental material (Fig. S1 and S2 and Tables S1 and S2).

There was no change in the specific growth rate or maximum cell concentration of *T. paralvinellae* when it was grown with or without *M. jannaschii* or with a change in carbon source (Fig. 2A and Fig. S2). The specific growth rates of *T. paralvinellae* grown on maltose in monoculture and in coculture were 0.16 ± 0.01 h^{-1} and 0.22 ± 0.02 h^{-1}, respectively, while growth rates on formate in monoculture and in coculture were 0.18 ± 0.05 h^{-1} and 0.16 ± 0.02 h^{-1}, respectively (Fig. 2A). Furthermore, when grown on maltose, there was no change in the growth yield (Table S3) or cell-specific acetate production rate of *T. paralvinellae* when grown in monoculture (0.94 ± 0.16 pmol cell^{-1} h^{-1}) relative to growth in coculture (1.05 ± 0.15 pmol cell^{-1} h^{-1}) (Fig. 2B). However, when grown on maltose, *T. paralvinellae* produced formate (in addition to H_2 and acetate) when grown in monoculture (0.60 ± 0.18 pmol cell^{-1} h^{-1}) but not when grown in coculture (Fig. 2C). The cell-specific H_2 production rate was higher when *T. paralvinellae* was grown in monoculture on formate (130.9 ± 11.1 fmol cell^{-1} h^{-1}) than for monoculture growth on maltose (0.9 ± 0.1 fmol cell^{-1} h^{-1}) (Table S3). A summary of the growth and metabolite production kinetics data for *T. paralvinellae* is available in the supplemental material (Fig. S2 and Table S3). There was no growth of *M. jannaschii* when it was incubated in monoculture in medium supplemented with only 0.01% yeast extract or 0.1% sodium formate and 0.01% yeast extract with N_2:CO_2 in the headspace. These additions also did not stimulate the growth of *M. jannaschii* in monoculture when an H_2:CO_2 headspace was provided.

Carbon isotope fractionation. The final carbon isotopic composition ($\delta^{13}C_{CO2}$) values were −24.4 to −21.6‰ in the coculture bottles and −33.3 to −28.2‰ in the

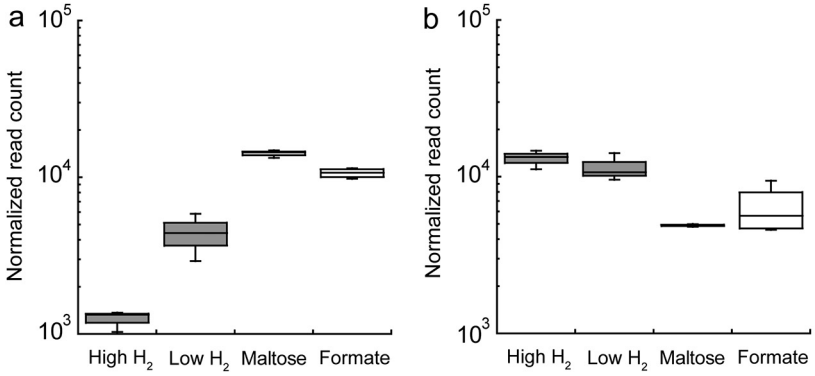

FIG 3 *M. jannaschii* transcript levels (relative log expression [RLE] normalization) for F_{420}-dependent methylene-H_4MPT dehydrogenase (*mtd*, MJ_RS05555) (a) and H_2-dependent methylene-H_4MPT I (*hmd*, MJ_RS04180) (b) for each growth condition.

chemostat (Table 1). The final $\delta^{13}C_{CO2}$ values of the *M. jannaschii* monocultures in bottles were +19.2 to +22.6‰, demonstrating a substantial drawdown of the reactant. $\delta^{13}C_{CH4}$ values became increasingly negative with increasing H_2 limitation during cell growth. The $\delta^{13}C_{CH4}$ values in the chemostat were −55.9 to −55.8‰ when *M. jannaschii* was grown on 80 to 83 μM H_2 and decreased to −75.7 to −72.5‰ when grown on 15 to 27 μM H_2. The corresponding values for isotopic fractionation of CO_2 to CH_4 ($\varepsilon_{CO2\text{-}CH4}$) increased from 28.5 to 29.3‰ during high H_2 growth to 43.7 to 45.9‰ during low H_2 growth (Table 1). Similarly, $\delta^{13}C_{CH4}$ values became more negative with increasing H_2 limitation during coculture cell growth. In monoculture with 1.92 atm of initial H_2 in the headspace at 82°C, the $\delta^{13}C_{CH4}$ from *M. jannaschii* was −34.2 to −32.9‰ (Table 1). $\delta^{13}C_{CH4}$ values decreased to −91.2 to −89.0‰ when *M. jannaschii* was grown in coculture with *T. paralvinellae* on maltose and to −99.4‰ when grown in coculture on formate. The corresponding $\varepsilon_{CO2\text{-}CH4}$ values increased from 22.1 to 23.0‰ during monoculture growth in a serum bottle to 73.5 to 85.1‰ during growth in coculture with *T. paralvinellae* (Table 1).

Transcriptomic analyses. RNA-Seq mapped 1,866 transcripts to the *M. jannaschii* genome. The thirteen samples that span four growth conditions were analyzed based on principal-component analysis (PCA) (Fig. S3A) and *t*-distributed stochastic neighbor embedding (*t*-SNE) (Fig. S3B) results. Pairwise comparisons of *M. jannaschii* grown in monoculture on high and low H_2 showed up to 12 genes to be differentially expressed (adjusted *P* value of <0.01 and $\log_2$ fold change [$|\log_2 FC|$] of >1) with 1 gene downregulated and 11 genes upregulated during growth on low H_2 relative to growth on high H_2 (Table S4). Under low-H_2 conditions, F_{420}-dependent methylene-tetrahydromethanopterin (H_4MPT) dehydrogenase (*mtd*, MJ_RS0555 in the NCBI RefSeq database) gene expression increased 3.5-fold (Fig. 3A). There was no significant change in gene expression for H_2-dependent methylene-H_4MPT dehydrogenases (*hmd*, MJ_RS04180; *hmdX*, MJ_RS03820) (Fig. 3B and Fig. S4) or for any of the methyl-coenzyme M (CoM) reductase A I or II genes (*mcrA*, MJ_RS00415 and MJ_RS04540) (Fig. S5) for *M. jannaschii* grown in monoculture on high and low H_2 in the chemostat. The genes that code for a GTP binding protein (MJ_RS01180), bacteriohemerythrin (MJ_RS03980), radical SAM protein (MJ_RS04390), a signal recognition particle (MJ_RS05550), a transcriptional regulator (MJ_RS06225), and four hypothetical proteins were upregulated on low H_2, while a gene that codes for a histone (MJ_RS04990) was upregulated on high H_2 (Table S4).

For cocultures grown on maltose, 97% of the reads mapped unambiguously to the *T. paralvinellae* genome and 1.5% mapped to the *M. jannaschii* genome. For cocultures grown on formate, 67% of the reads mapped unambiguously to the *T. paralvinellae* genome and 29% mapped to the *M. jannaschii* genome. These proportions generally matched the proportions of *T. paralvinellae* and *M. jannaschii* cells in each coculture

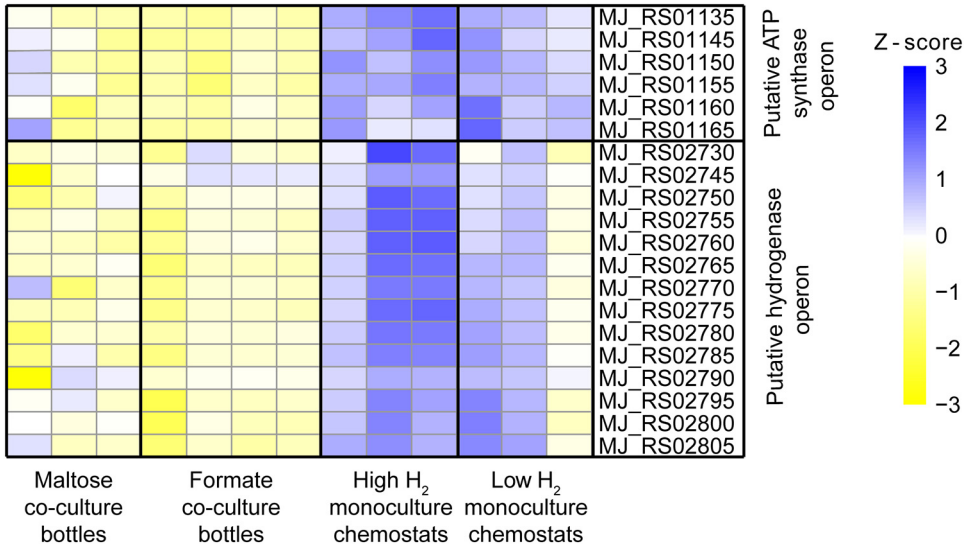

FIG 4 Differential gene expression analysis and RNA-Seq heat map for the *M. jannaschii* putative ATP synthase operon (MJ_RS01135 and MJ_RS01145 to MJ_RS01165) and the *M. jannaschii* putative hydrogenase operon (MJ_RS02730 and MJ_RS02745 to MJ_RS02805) for each growth condition.

type based on cell concentration estimates (Fig. S2). Merged pairwise comparisons of *M. jannaschii* gene expression for cultures grown in monoculture and *M. jannaschii* grown in coculture with *T. paralvinellae* showed up to 338 genes to be differentially expressed (adjusted *P* value of <0.01 and $|\log_2 FC|$ of >1) with 146 upregulated genes and 192 downregulated genes when grown in coculture relative to growth in monoculture on high and low H_2 (Table S5). However, we cannot rule out the possibility that some of these gene expression changes are caused by the switch from the chemostat to bottles.

F_{420}-dependent methylene-H_4MPT dehydrogenase (*mtd*, MJ_RS05555) gene expression was upregulated 4.3-fold in coculture relative to that of *M. jannaschii* grown under monoculture conditions (Fig. 3A). In contrast, gene expression of H_2-dependent methylene-H_4MPT dehydrogenases (*hmd*, MJ_RS04180; *hmdX*, MJ_RS03820) were both downregulated 2.1-fold in *M. jannaschii* grown in coculture relative to that of *M. jannaschii* grown in monoculture (Fig. 3B and Fig. S4). There was no change in gene expression for the methyl-CoM reductase I and II genes (Fig. S5). Gene expression for a hypothetical protein with a predicted RNA-binding domain (MJ_RS03480) showed a 22.5-fold increase in cocultures relative to monocultures (Fig. S6). Expression of 6 of the 9 *M. jannaschii* genes that code for a V-type ATP synthase (MJ_RS01130 to MJ_RS01165 and MJ_RS03255) were downregulated when cultures were grown in coculture relative to expression in *M. jannaschii* grown in monoculture (Fig. 4). Similarly, expression of 14 genes in a putative operon for membrane-bound, ferredoxin-dependent hydrogenase was also downregulated in *M. jannaschii* cultures grown in cocultures relative to cultures grown in monoculture (Fig. 4). These genes include Eha subunits A and B (MJ_RS02795 to MJ_RS02800), an oxidoreductase (MJ_RS02755), a dehydrogenase (MJ_RS02765), and a catalytic subunit (MJ_RS02730).

DISCUSSION

Microorganisms in nature live in complex communities and biogeochemically impact their environment through interspecies metabolic interactions. Most of what is known about the kinetics and physiology of methanogenesis at various H_2 concentrations and in coculture comes from studies of the thermophile *Methanothermobacter thermoautotrophicus* and the mesophile *Methanococcus maripaludis*. Growth rates of both organisms decreased when they were H_2 limited relative to H_2-replete growth. However, growth yields (Y_{CH4}) increased when the cultures were H_2 limited (26–28).

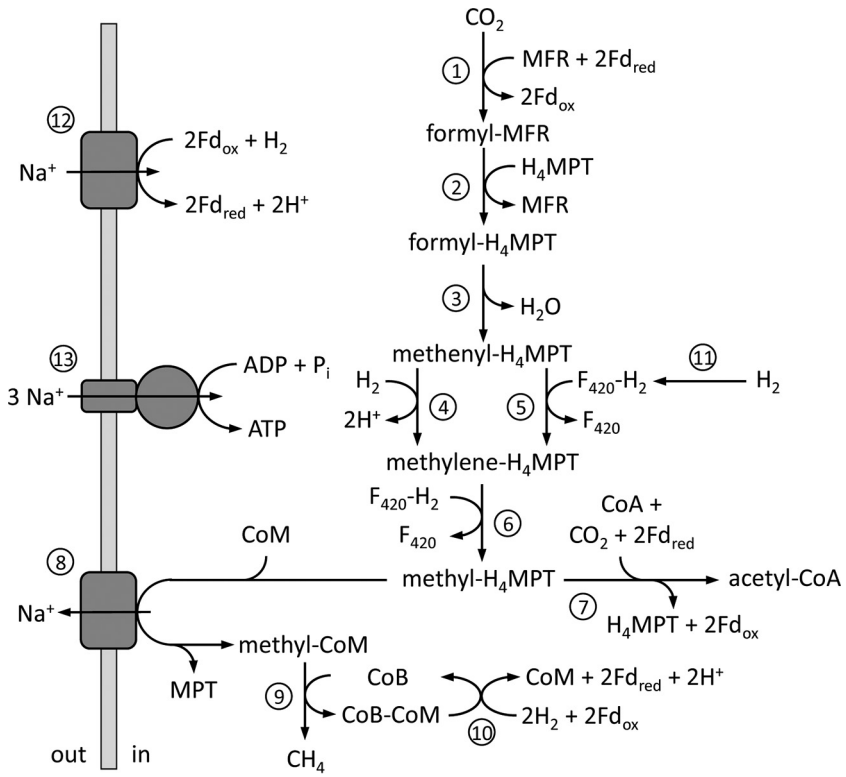

FIG 5 General metabolic pathway for *M. jannaschii*. The enzymes are (1) formylmethanofuran dehydrogenase, (2) formylmethanofuran:H_4MPT formyltransferase, (3) cyclohydrolase, (4) H_2-dependent methylene-H_4MPT dehydrogenase (Hmd), (5) F_{420}-dependent methylene-H_4MPT dehydrogenase (Mtd), (6) methylene-H_4MPT reductase (Mer), (7) CO dehydrogenase/acetyl-CoA synthase, (8) methyl-H_4MPT:CoM methyltransferase, (9) methyl-CoM reductase (Mcr), (10) hydrogenase-heterodisulfide reductase complex, (11) F_{420}-dependent hydrogenase, (12) membrane-bound ferredoxin-dependent hydrogenase, and (13) membrane-bound ATP synthase. MFR, methanofuran; H_4MPT, tetrahydromethanopterin; F_{420}, electron carrier coenzyme F_{420}; CoA, coenzyme A; CoM, coenzyme M; CoB, coenzyme B; and Fd, electron carrier ferredoxin.

Prior to this study, growth yields had not been measured for any methanogen during interspecies H_2 transfer or for any hyperthermophilic methanogens under various H_2 concentrations.

To determine *M. jannaschii* metabolism and kinetics under H_2-replete and H_2-limited growth conditions, as defined in a previous study (9), continuous growth in chemostats was established. The decrease in specific growth rate and cell-specific CH_4 production rate of *M. jannaschii* when grown in monoculture under H_2-limited conditions show that growth and methanogenesis rates are limited by H_2 concentration. This trend continued when *M. jannaschii* was grown in coculture with *T. paralvinellae*, suggesting that interspecies H_2 transfer led to further H_2 limitation of methanogenesis. However, the cell yield for *M. jannaschii* increased when the cells were grown in coculture relative to growth in monoculture. This is consistent with previous studies that show higher cell yields for *M. thermoautotrophicus* and *M. maripaludis* upon H_2 limitation, but there is no consensus on a physiological explanation (26–28). During methanogenesis, methyl-H_4MPT is either converted to methyl-CoM for production of CH_4 and energy generation on the cytoplasmic membrane or to acetyl-CoA for biosynthetic reactions (Fig. 5). Depending on the H_2 concentration, hydrogenotrophic methanogens decide between maximum growth rate and maximum growth yield. This pattern can be explained by the rate-yield trade-off, which creates two divergent ecological strategies, namely, (i) slow growth but efficient metabolism and high yields when resources are scarce, and (ii) fast growth but inefficient metabolism and low yields upon rich resources. The rate-yield trade-off is suggested to be integral to evolution and the coexistence of

species (29). It was proposed previously but not demonstrated that syntrophic growth of methanogens with a fermentative partner is optimized for cell yield rather that growth rate (27). In this study, *M. jannaschii* grew and produced CH_4 solely on the H_2 produced by *T. paralvinellae*, and the cell yield of *M. jannaschii* increased in coculture compared to that of growth in monoculture.

Thermococcus species use maltose for biosynthesis and energy generation that yields acetate and CO_2 as well as H_2 and a proton/sodium-motive force via a membrane-bound hydrogenase (30, 31). However, they are auxotrophic for certain amino acids that must be supplied from the environment (32, 33). *T. paralvinellae* increased gene expression of a membrane-bound formate hydrogenlyase operon and produced formate when inhibited by exogenous H_2, suggesting that it converts H_2 to formate when H_2 is inhibited (22). *T. paralvinellae* also separately used formate as an energy source in the absence of maltose, produced H_2, and generated a proton/sodium-motive force but required 0.01% yeast extract in the growth medium (22). Consequently, the cell-specific H_2 production rate was ~100-fold higher when cultures were grown on formate.

Morris et al. (34) defined microbial syntrophy as obligately mutualistic metabolism and included coculture growth between the hyperthermophilic H_2 producer *Pyrococcus furiosus* and various hyperthermophilic methanogens, including *M. jannaschii*, as an example based on increased cell concentrations of both organisms in coculture relative to each in monoculture (35). Unlike *T. paralvinellae*, *P. furiosus* lacks formate hydrogenlyase as a mechanism to overcome H_2 inhibition (36) and may be more dependent upon syntrophy to ameliorate H_2 inhibition. In this study, when *T. paralvinellae* was grown with *M. jannaschii*, growth in coculture did not stimulate the growth rate, growth yield, or maximum cell concentration of *T. paralvinellae*. This suggests the relationship between *T. paralvinellae* and *M. jannaschii* is not obligately mutualistic and therefore more accurately represents interspecies H_2 transfer rather than syntrophy. However, there was no formate production when *T. paralvinellae* was grown in coculture on maltose with *M. jannaschii*, and *M. jannaschii* cannot grow on formate (37 and this study), so *M. jannaschii* does appear to ameliorate H_2 inhibition in *T. paralvinellae* when grown in coculture.

It was shown previously that the fractionation of carbon isotopes between CO_2 and CH_4 increased with decreasing concentrations of H_2 availability or, more accurately, with decreasing Gibbs energy for the methanogenesis reaction (23). The $\varepsilon_{CO2\text{-}CH4}$ fractionation factor for the thermophile *Methanothermobacter marburgensis* increased from 22 to 39‰ at high H_2 concentrations to 58 to 64‰ at limiting H_2 concentrations (23, 24). It was proposed that variations in the carbon isotopic fractionation factor are controlled by the extent of reversibility of the methanogenesis pathway, which was proposed to increase with decreasing Gibbs energy availability (23). In this study, the CH_4 produced was isotopically more negative and the $\varepsilon_{CO2\text{-}CH4}$ fractionation factor increased when *M. jannaschii* was grown in the chemostat with low H_2 relative to high H_2 conditions. Similarly, in bottles, CH_4 was isotopically more negative and $\varepsilon_{CO2\text{-}CH4}$ was much larger when *M. jannaschii* was grown in coculture with *T. paralvinellae* than when it was grown in monoculture with an initial estimated aqueous H_2 concentration of 1.2 mM. The most negative CH_4 in this study was produced when *M. jannaschii* was grown in coculture and H_2 fluxes are presumably at their lowest rates.

Previous studies showed that during CO_2 fixation and methanogenesis (Fig. 5) in *M. thermoautotrophicus* and *M. maripaludis*, gene expression for H_2-dependent methylene-H_4MPT dehydrogenase (*hmd*) decreased while expression of cofactor F_{420}-dependent methylene-H_4MPT (*mtd*) increased when growth was H_2 limited relative to that of H_2-replete growth (27, 28, 38). It was suggested that the Mtd reaction is the more reversible of the two methylene-H_4MPT dehydrogenase reactions, which facilitates enhanced carbon isotope fractionation by methanogenesis pathway reversal in these methanogens under H_2-limited conditions (23). The proteome of *M. jannaschii* contained a lower abundance of Hmd and higher abundances of Mtd and four flagellar proteins in early logarithmic growth phase when grown in batch phase under H_2-

limited conditions than under H_2-replete conditions, but both Hmd and Mtd were found at high relative abundances in late logarithmic growth phase when grown under H_2-replete conditions (39). During H_2 syntrophy, the *M. thermoautotrophicus* proteome had more Mtd and less Hmd than were seen with monoculture growth under H_2-replete conditions (40). There were no significant changes in gene expression or protein abundance for Hmd and Mtd in *M. maripaludis* during H_2 syntrophy relative to that of an H_2-limited monoculture (41).

In this study, RNA-Seq was used to determine changes in gene expression profiles in *M. jannaschii* for carbon assimilation, CH_4 production, and energy generation pathways when there were changes in H_2 availability. When *M. jannaschii* was grown under H_2-limited conditions and in coculture, *mtd* expression was significantly upregulated and *hmd* expression was significantly downregulated in coculture cells compared to that of monoculture cells. This suggests a preference for F_{420} as an electron carrier in the methanogenesis pathway under H_2-limited conditions. The increase in cell yield in coculture was not supported by a change in the expression of genes in the carbon assimilation and methanogenesis pathways. No significant changes were detected in the expression of methyl-CoM reductase I and II and methyl-H_4MPT:CoM methyltransferase, which catalyze the last two steps of methanogenesis (Fig. 5). Previously, changes in the relative abundances of methyl-CoM reductases I and II were observed in *M. thermoautotrophicus* with H_2 availability and growth during syntrophy (27, 40, 42). Moreover, there was no change in expression in our study in the carbon monoxide dehydrogenase/acetyl-CoA synthase genes, which code for the enzyme that converts methyl-MPT to acetyl-CoA.

In coculture, there was up to a 22.5-fold increase in the expression of a putative RNA binding protein that is only found in methanogens and the *Thermococcales* and has been proposed to regulate cellular activity at the translation level (43). The decrease in the expression of genes in the putative membrane-bound, ferredoxin-dependent hydrogenase operon and in the membrane-bound, Na^+-translocating V-type ATPase operon supports the kinetic observations that *M. jannaschii* is energy limited when grown in coculture. Under H_2-limited coculture conditions, the cell must direct more of its methyl-H_4MPT toward biosynthesis. Furthermore, there was no change in the expression of the genes for flagella. This was different from what was previously observed for *M. jannaschii* using proteomics (39) and may be due to the use of a chemostat in this study instead of a batch reactor.

In environments such as low-H_2 hydrothermal vents along subduction zones and some mid-ocean ridges, oil reservoirs, and high saline shale beds where organic compounds are present and H_2 efflux rates are low, thermophilic methanogens like *M. jannaschii* likely can grow and produce CH_4 through interspecies H_2 transfer with hyperthermophilic H_2-producing heterotrophs, like *T. paralvinellae*, with high cell yields and large carbon isotope fractionations, but they do so at very low rates. This likely explains the presence of thermophilic H_2 producers and thermophilic, hydrogenotrophic methanogens in petroleum reservoirs and may be a source of CH_4 in that habitat. In contrast, high-temperature methanogens in high-H_2 hydrothermal vents, such as those supported by serpentinization and following volcanic eruptions (2), may subsist entirely from abiotic H_2 with elevated cell-specific CH_4 production rates and smaller carbon isotope fractionations. Metatranscriptomic analyses coupled with carbon isotope analyses of native CH_4 will help to determine what fraction of methanogenesis in a high-temperature environment is due to interspecies H_2 transfer relative to growth on abiotic H_2. In this manner, we will be better equipped to model cooperative, competitive, and neutral interactions between different species in an environment and predict the biogeochemical outcome of a mixed community living in a habitat.

MATERIALS AND METHODS

Growth media and culture conditions. *Methanocaldococcus jannaschii* DSM 2661 (37) and *Thermococcus paralvinellae* DSM 27261 (44) were purchased from the Deutsche Sammlung von Mikroorganismen und Zellkulturen (DSMZ). The growth medium for pure cultures of *M. jannaschii* was based on DSM medium 282 (9). For the cocultures of *M. jannaschii* and *T. paralvinellae* and monoculture of *T.*

paralvinellae, the base medium was amended with 0.01% (wt vol^{-1}) yeast extract (vitamin B_{12} fortified; Difco), 1 μM $Na_2WO_4{\cdot}2H_2O$, 0.26 μM $(NH_4)_2Fe(SO_4)_2{\cdot}6H_2O$, and 0.25 μM $(NH_4)_2Ni(SO_4)_2{\cdot}6H_2O$. The primary carbon and energy source added for *T. paralvinellae* was either 0.5% (wt vol^{-1}) maltose (Sigma) or 0.1% (wt vol^{-1}) sodium formate (Fluka). All media were pH balanced to 6.00 $\pm$ 0.05 and reduced with 0.025% (wt vol^{-1}) each of cysteine-HCl and $Na_2S{\cdot}9H_2O$ before inoculation. To test if *M. jannaschii* can use formate or yeast extract for growth in the absence of H_2, or if they stimulate growth in the presence of H_2, *M. jannaschii* was incubated in monoculture on the base medium amended with 0.1% formate and 0.01% yeast extract or 0.01% yeast extract only as described above, each in serum bottles with 1 additional atm (100 kPa) of either H_2:CO_2 (80%:20%) or N_2:CO_2 (80%:20%) added to the headspace at room temperature prior to incubation.

M. jannaschii was grown in monoculture at 82°C and under high and low H_2 concentrations in a chemostat to measure its growth and CH_4 production kinetics and to generate biomass for gene expression analysis. A 2-liter bioreactor (all-in-one benchtop reactor; Ace Glass) with gas flow, temperature ($\pm$0.1°C), and pH ($\pm$0.1 unit; Eutech Instruments pH 200 Series) controls was used with 1.5 liters of growth medium. The medium was maintained at pH 6.0 $\pm$ 0.1 by the automatic addition of 0.25 mM HCl. For high-H_2 conditions, the bioreactor was gassed with a mixture of CO_2 (20.5 ml min^{-1}) and H_2 (132 ml min^{-1}). For low-H_2 conditions, the bioreactor was gassed with a mixture of CO_2 (20.5 ml min^{-1}), N_2 (130 ml of gas min^{-1}), and H_2 (2.5 ml min^{-1}). Pure gases were blended using a mass flow controller (Matheson Tri-Gas) and added to the bioreactor through a single submerged fritted bubbler (70 to 100 μm; Ace Glass; ASTM certified). The reactor is an open system and remains at ambient gas pressure. It was stirred at 150 to 180 rpm using a four-blade open impeller (6-cm diameter) with a glass shaft and Teflon blades. Aqueous H_2 and CH_4 concentrations were measured before and after inoculation by drawing 25 ml of medium from the bottom of the bioreactor directly into anoxic 60-ml serum bottles and measuring the headspace gas. H_2 was measured using a gas chromatograph fitted with a thermal conductivity detector (Shimadzu GC-8A) and a 60/80 Carboxen 1000 column (15 feet by 1/8 inch; Supelco). CH_4 was measured using a gas chromatograph fitted with a flame ionization detector (Shimadzu GC-17A) and a 5A 80/100 molecular sieve column (6 feet by 1/8 inch; Alltech). The aqueous H_2 concentrations in the bioreactor prior to inoculation were 80 to 83 μM for the high-H_2 condition and 15 to 27 μM for the low-H_2 condition (Table 1).

The media were inoculated with 50 to 100 ml of a logarithmic-growth-phase culture of *M. jannaschii*. During growth, liquid samples were drawn from the bioreactor and cell concentrations were determined using phase-contrast light microscopy and a Petroff-Hausser counting chamber. The growth rate (k) was determined by plotting cell concentration against time and fitting a logarithmic curve to the growth data. *M. jannaschii* was grown in batch reactor mode until the culture reached mid-logarithmic growth phase, and then the bioreactor was switched to chemostat mode by pumping sterile growth medium into the bioreactor from a sealed 12-liter reservoir that was degassed with N_2 through a submerged glass tube and heated to 75°C. Simultaneously and at the same rate, spent growth medium was pumped out of the bioreactor using a dual-channel peristaltic pump. The H_2 and CH_4 concentrations in the headspace of the bioreactor were measured using gas chromatography as described above. At high and low H_2 concentrations, cells were grown in the reactor at low enough cell concentrations such that there was excess H_2 in the headspace and the cells were not H_2 limited (see Fig. S1 in the supplemental material).

Growth of *M. jannaschii* was stable in the chemostat after three volume replacements of the medium within the reactor ($\sim$5 h for high H_2, $\sim$14 h for low H_2) and was monitored for an additional $\sim$0.5 volume replacements to obtain kinetic data. The CH_4 production rate per cell (q) was calculated from the sum of the CH_4 concentration in the headspace times the gas flow rate and the CH_4 concentration in the medium times the medium dilution rate (i.e., CH_4 production rate), which was normalized by the total cell concentration in the reactor. The cell yield per mole of CH_4 produced (Y_{CH4}) was calculated by dividing the cell production rate (dilution rate times cell concentration) by the CH_4 production rate. The complete contents of the bioreactor then were drained into ice-cooled centrifuge bottles, spun in a centrifuge at 10,000 $\times$ g and 4°C for 60 min, resuspended in 1 ml of TRIzol (Invitrogen), and frozen at $-$80°C until processed. Chemostats were run in triplicate for both conditions.

M. jannaschii and *T. paralvinellae* were grown in coculture at 82°C in 2-liter gas-tight flasks (Pyrex bottles sealed with rubber lyophilization stoppers) containing 1.5 liters of medium with ambient pressure of N_2:CO_2 (80%:20%) in the headspace at room temperature without agitation and either maltose or formate as the energy source (Table 1). Separate logarithmic-growth-phase cultures of *M. jannaschii* and *T. paralvinellae* were combined to inoculate the bottles. The coculture was established immediately and did not require prior coculture transfers. At various times during growth, total cell concentration in bottles was determined using a Petroff-Hausser counting chamber and phase-contrast light microscopy. The *M. jannaschii* cell concentration was determined by counting the number of autofluorescent cells using epifluorescence microscopy and UV light excitation (45). The concentration of *T. paralvinellae* cells was calculated by subtracting the concentration of *M. jannaschii* cells from the total cell concentration. The pH change was $<$0.1 pH units during growth. For comparison, *T. paralvinellae* was grown separately in the same bottles and conditions in monoculture on 0.5% maltose and separately on 0.1% sodium formate, both with ambient pressure of N_2:CO_2 in the headspace at room temperature. Cell concentrations were measured as described above.

The growth rates (k) of *M. jannaschii* and *T. paralvinellae* were determined by plotting cell concentration against time and fitting a logarithmic curve to the growth data. The total amounts of CH_4 and H_2 in the bottles were determined by gas chromatography. The concentrations of formate, acetate, butyrate, isovalerate, and 2-methylbutyrate were measured from aliquots of syringe-filtered (0.2-μm pore size)

spent medium from each coculture and *T. paralvinellae* monoculture incubation at various time points (for maltose growth only) using ultra-high-pressure liquid chromatography (UHPLC) as previously described (46). Methanogen cell yields (Y_{CH4}) were determined from the linear slope of the number of methanogen cells per bottle plotted against the amount of CH_4 per bottle (47). The rate of CH_4 production per cell is calculated from $k/(0.693 \times Y_{CH4})$ as previously described (47). Similarly, *T. paralvinellae* cell yields based on acetate and formate produced and for H_2 produced (for monoculture only) were determined from the linear slope of *T. paralvinellae* cell concentration plotted against acetate, formate, or H_2 concentration. When the cocultures reached late logarithmic growth phase, the cells were harvested for transcriptome analysis as described above (*T. paralvinellae* cells were not harvested when grown in monoculture). Cocultures grown on maltose were grown in triplicate, while cocultures grown on formate were grown in quadruplicate.

Carbon isotope fractionation. At the start (T_o) and end (T_f) of each chemostat run, 20 ml of chemostat headspace was transferred in triplicate into evacuated vials (Labco Exetainer). *M. jannaschii* also was grown in monoculture in 245-ml serum bottles containing 100 ml of medium and 1 additional atm (100 kPa) of H_2:CO_2 (80%:20%) added to the headspace at room temperature prior to incubation. *M. jannaschii* was also grown in coculture with *T. paralvinellae* in 245-ml serum bottles containing 100 ml of either 0.5% maltose medium or 0.1% sodium formate medium as described above. The isotopic signatures of CH_4 were determined using a gas chromatography-combustion-isotope ratio mass spectrometer (GC-C-IRMS; Thermo Scientific) equipped with a GS-CarbonPlot column (30 m long, 0.320-mm inner diameter, 1.50-μm film thickness; Agilent). Isotopic signatures were determined using external CH_4 standards of known isotopic signatures (-57.40 ± 0.06‰) that were obtained from Arndt Schimmelmann (Indiana University). The error of the analysis was determined from external standards, and the standard deviation of multiple injections was 0.3‰. At T_o and T_f of the chemostat runs and the serum bottles, triplicate samples of dissolved inorganic carbon (DIC) were drawn from the growth medium. Each DIC sample (either 0.8 or 1.0 ml) was syringe filtered (0.2 μm pore size) and injected into prepared vials (Labco Exetainer) that had been flushed with He and contained 100 μl of phosphoric acid. Samples were analyzed by GasBench-IRMS. DIC standards were prepared in concentrations from 0.5 to 7.0 mM using $KHCO_3$ and Li_2CO_3 of known isotopic composition (-38.1‰ and -1.1‰, respectively). The error of analysis was determined from external standards, and the standard deviation of multiple injections was 0.3‰. The $\delta^{13}C_{CO2}$ value was calculated from the $\delta^{13}C_{DIC}$ value using the relationship of Mook et al. (48) at the temperature of the cultures (82°C).

Carbon isotopic compositions are presented as $\delta^{13}C$ in the per mille notation (‰) relative to the VPDB (Vienna Pee Dee Belemnite) standard:

$$\delta^{13}C = \left[\frac{R_{Sample}}{R_{Standard}}\right] - 1 \times 10^3 \left(‰\right) \quad (1)$$

where R_{sample} is the $^{13}C/^{12}C$ ratio of the sample and $R_{standard}$ is 0.0112372. The ε notation is used to express isotope fractionation factors in per mille (‰):

$$\varepsilon_{CO2-CH4} = \left(\alpha_{CO2-CH4} - 1\right) \times 10^3 \left(‰\right) \quad (2)$$

The fractionation factor, α, is defined as the ratio between the isotopic ratio in the substrate and product:

$$\alpha_{CO2-CH4} = \frac{R_{CO2}}{R_{CH4}} = \frac{\delta^{13}C_{CO2} + 10^3}{\delta^{13}C_{CH4} + 10^3} \quad (3)$$

where R_{CO2} is the $^{13}C/^{12}C$ ratio of the initial CO_2 and R_{CH4} is the $^{13}C/^{12}C$ ratio of the CH_4 produced. The propagated error of the fractionation factors was 0.4‰, except in the case of the *M. jannaschii* monoculture.

The inorganic carbon in the *M. jannaschii* monoculture serum bottles was extensively drawn down, substantially altering the ^{13}C signature of the remaining reactant. The fractionation factor was therefore calculated by setting the initial CO_2 isotopic signature equal to that in serum bottles without cells (-26.1 ± 0.8‰) and reacting it stepwise under different fractionation factors. To obtain final isotopic compositions that match the remaining CO_2 ($+18.9$ and $+15.5$‰) and the final accumulated product, CH_4 (-32.9‰ and -34.2‰), fractionation factors of 22.1 ± 1.3‰ and 23.0 ± 1.3‰ were required in the two different experiments.

RNA-Seq analysis. Total RNA was extracted from 13 cell pellets from each growth condition (Table 1) using a Direct-zol RNA extraction kit (Zymo). RNA quantity was determined using Qubit fluorometry. RNA integrity was checked using an Agilent 2100 bioanalyzer, a NanoDrop 2000 spectrophotometer, and gel electrophoresis of the RNA, followed by staining with ethidium bromide. Removal of rRNA, library construction, multiplexing, and sequencing of the mRNA using an Illumina HiSeq2500 sequencer with two 150-bp paired ends was performed commercially by GENEWIZ, LLC (South Plainfield, NJ, USA), as described by the company. Sequencing depths ranged from 30,751,946 to 41,634,527 sequence reads per sample, with a median of 34,532,231 and a mean of 35,155,474 reads per sample. The RNA-Seq reads were mapped to both *M. jannaschii* and *T. paralvinellae* genomes using BBSplit from the BBMap package (https://sourceforge.net/projects/bbmap/). BBSplit is an aligner tool that bins sequencing reads by mapping them to multiple references simultaneously and separates the reads that map to multiple references to a special "ambiguous" file for each of them. For further analyses, we removed all ambiguously mapped reads to both genomes and worked with only the reads that unambiguously map to the *M. jannaschii* genome. Two to 5% of the reads were lost in this step.

The mapped reads for *M. jannaschii* were aligned to the *M. jannaschii* genome and sorted using the STAR aligner, version 2.5.1b (49). Aligned sequence reads were assigned to genomic features and

quantified using the featureCounts read summarization tool (50). The output of the analyses generated BAM files containing the sequence of every mapped read and its mapped location. An unsupervised *t*-SNE algorithm (51) and PCA were used to predict outliers among the total RNA sample replicates.

Genes that were differentially expressed were identified using DESeq2 in the Bioconductor software framework (https://www.bioconductor.org) in R (version 3.3 [http://www.r-project.org]) and on a Galaxy platform using DEBrowser (52–55). Relative log expression normalization was performed by using the R package DESeq2. The DESeq2 package allows for sequencing depth normalization between samples, estimates gene-wise dispersion across all samples, fits a negative binomial generalized linear model, and applies Wald statistics to each gene. The genes were reported as differentially regulated if the $|\log_2 FC|$ value was >1 and the adjusted P value was <0.01. Heatmaps were plotted in R (version 3.3 [http://www.r-project.org]) using the pheatmap package. The heatmap color scale represents the z-score, which is the number of standard deviations the mean score of the treatment is from the mean score of the entire population.

Data availability. The count files and raw sequences are available in the NCBI Gene Expression Omnibus (GEO) database under accession no. GSE112986.

SUPPLEMENTAL MATERIAL

Supplemental material for this article may be found at https://doi.org/10.1128/AEM.00180-19.

SUPPLEMENTAL FILE 1, PDF file, 1.2 MB.

ACKNOWLEDGMENT

We thank Elif Yildirim and Srishti Kashyap for their assistance. This work was funded by grants to J.F.H. from the USDA National Institute of Food and Agriculture (grant MAS00489) and by the Gordon and Betty Moore Foundation (grant GBMF 3297). Funding for the isotope analyses was provided by grants to S.Q.L. from the Center for Dark Energy Biosphere Investigations (C-DEBI) and the National Science Foundation (NSF-EAR/IF-1349539). We have no conflict of interest to declare. B.D.T. and J.F.H. conceived and designed the study, conducted the growth and gene expression experiments, and wrote the paper. B.D.T. and C.M. conducted the gene expression analyses, and T.B.N. and S.Q.L. conducted the carbon isotope analyses. All authors analyzed the data and read and approved the final manuscript.

REFERENCES

1. Thauer RK, Kaster AK, Seedorf H, Buckel W, Hedderich R. 2008. Methanogenic archaea: ecologically relevant differences in energy conservation. Nat Rev Microbiol 6:579–591. https://doi.org/10.1038/nrmicro1931.
2. Holden JF, Breier JA, Rogers KL, Schulte MD, Toner BM. 2012. Biogeochemical processes at hydrothermal vents: microbes and minerals, bioenergetics, and carbon fluxes. Oceanography 25:196–208. https://doi.org/10.5670/oceanog.2012.18.
3. LaRowe DE, Burwicz E, Arndt S, Dale AW, Amend JP. 2017. Temperature and volume of global marine sediments. Geology 45:275–278. https://doi.org/10.1130/G38601.1.
4. Davidova IA, Duncan KE, Perez-Ibarra BM, Suflita JM. 2012. Involvement of thermophilic archaea in the biocorrosion of oil pipelines. Environ Microbiol 14:1762–1771. https://doi.org/10.1111/j.1462-2920.2012.02721.x.
5. Topçuoğlu BD, Stewart LC, Morrison HG, Butterfield DA, Huber JA, Holden JF. 2016. Hydrogen limitation and syntrophic growth among natural assemblages of thermophilic methanogens at deep-sea hydrothermal vents. Front Microbiol 7:1240. https://doi.org/10.3389/fmicb.2016.01240.
6. Takai K, Gamo T, Tsunogai U, Nakayama N, Hirayama H, Nealson KH, Horikoshi K. 2004. Geochemical and microbiological evidence for a hydrogen-based, hyperthermophilic subsurface lithoautotrophic microbial ecosystem (HyperSLiME) beneath an active deep-sea hydrothermal field. Extremophiles 8:269–282. https://doi.org/10.1007/s00792-004-0386-3.
7. Nakagawa S, Takai K, Inagaki F, Chiba H, Ishibashi J, Kataoka S, Hirayama H, Nunoura T, Horikoshi K, Sako Y. 2005. Variability in microbial community and venting chemistry in a sediment-hosted backarc hydrothermal system: impacts of subseafloor phase-separation. FEMS Microbiol Ecol 54:141–155. https://doi.org/10.1016/j.femsec.2005.03.007.
8. Flores GE, Campbell JH, Kirshtein JD, Meneghin J, Podar M, Steinberg JI, Seewald JS, Tivey MK, Voytek MA, Yang ZK, Reysenbach AL. 2011. Microbial community structure of hydrothermal deposits from geochemically different vent fields along the Mid-Atlantic Ridge. Environ Microbiol 13:2158–2171. https://doi.org/10.1111/j.1462-2920.2011.02463.x.
9. Ver Eecke HC, Butterfield DA, Huber JA, Lilley MD, Olson EJ, Roe KK, Evans LJ, Merkel AY, Cantin HV, Holden JF. 2012. Hydrogen-limited growth of hyperthermophilic methanogens at deep-sea hydrothermal vents. Proc Natl Acad Sci U S A 109:13674–13679. https://doi.org/10.1073/pnas.1206632109.
10. Reveillaud J, Reddington E, McDermott J, Algar C, Meyer JL, Sylva S, Seewald J, German CR, Huber JA. 2016. Subseafloor microbial communities in hydrogen-rich vent fluids from hydrothermal systems along the Mid-Cayman Rise. Environ Microbiol 18:1970–1987. https://doi.org/10.1111/1462-2920.13173.
11. Fortunato CS, Larson B, Butterfield DA, Huber JA. 2018. Spatially distinct, temporally stable microbial populations mediate biogeochemical cycling at and below the seafloor in hydrothermal vent fluids. Environ Microbiol 20:769–784. https://doi.org/10.1111/1462-2920.14011.
12. Orphan VJ, Taylor LT, Hafenbradl D, DeLong EF. 2000. Culture-dependent and culture-independent characterization of microbial assemblages associated with high-temperature petroleum reservoirs. Appl Environ Microbiol 66:700–711. https://doi.org/10.1128/AEM.66.2.700-711.2000.
13. Bonch-Osmolovskaya EA, Miroshnichenko ML, Lebedinsky AV, Chernyh NA, Nazina TN, Ivoilov VS, Belyaev SS, Boulygina ES, Lysov YP, Perov AN, Mirzabekov AD, Hippe H, Stackebrandt E, L'Haridon S, Jeanthon C. 2003. Radioisotopic, culture-based, and oligonucleotide microchip analyses of thermophilic microbial communities in a continental high-temperature petroleum reservoir. Appl Environ Microbiol 69:6143–6151. https://doi.org/10.1128/AEM.69.10.6143-6151.2003.

14. Nazina TN, Shestakova NM, Grigor'yan AA, Mikhailova EM, Tourova TP, Poltaraus AB, Feng C, Ni F, Belyaev SS. 2006. Phylogenetic diversity and activity of anaerobic microorganisms of high-temperature horizons of the Dagang oil field (P. R. China). Microbiology 75:55–65. https://doi.org/10.1134/S0026261706010115.
15. Dahle H, Garshol F, Madsen M, Birkeland NK. 2008. Microbial community structure analysis of produced water from a high-temperature North Sea oil-field. Antonie Van Leeuwenhoek 93:37–49. https://doi.org/10.1007/s10482-007-9177-z.
16. Kotlar HK, Lewin A, Johansen J, Throne-Holst M, Haverkamp T, Markussen S, Winnberg A, Ringrose P, Aakvik T, Ryeng E, Jakobsen K, Drabløs F, Valla S. 2011. High coverage sequencing of DNA from microorganisms living in an oil reservoir 2.5 kilometres subsurface. Environ Microbiol Rep 3:674–681. https://doi.org/10.1111/j.1758-2229.2011.00279.x.
17. Lewin A, Johansen J, Wentzel A, Kotlar HK, Drabløs F, Valla S. 2014. The microbial communities in two apparently physically separated deep subsurface oil reservoirs show extensive DNA sequence similarities. Environ Microbiol 16:545–558. https://doi.org/10.1111/1462-2920.12181.
18. Junzhang L, Bin H, Gongzhe C, Jing W, Yun F, Xiaoming T, Weidong W. 2014. A study on the microbial community structure in oil reservoirs developed by water flooding. J Petrol Sci Eng 122:354–359. https://doi.org/10.1016/j.petrol.2014.07.030.
19. Okpala GN, Chen C, Fida T, Voordouw G. 2017. Effect of thermophilic nitrate reduction of sulfide production in high temperature oil reservoir samples. Front Microbiol 8:1573. https://doi.org/10.3389/fmicb.2017.01573.
20. Ehrhardt CJ, Haymon RM, Lamontagne MG, Holden PA. 2007. Evidence for hydrothermal Archaea within the basaltic flanks of the East Pacific Rise. Environ Microbiol 9:900–912. https://doi.org/10.1111/j.1462-2920.2006.01211.x.
21. Dolfing J, Larter SR, Head IM. 2008. Thermodynamic constraints on methanogenic crude oil biodegradation. ISME J 2:442–452. https://doi.org/10.1038/ismej.2007.111.
22. Topçuoğlu BD, Meydan C, Orellana R, Holden JF. 2018. Formate hydrogenlyase and formate secretion ameliorate H_2 inhibition in the hyperthermophilic archaeon *Thermococcus paralvinellae*. Environ Microbiol 20:949–957. https://doi.org/10.1111/1462-2920.14022.
23. Valentine DL, Chidthaisong A, Rice A, Reeburgh WS, Tyler SC. 2004. Carbon and hydrogen isotope fractionation by moderately thermophilic methanogens. Geochim Cosmochim Acta 68:1571–1590. https://doi.org/10.1016/j.gca.2003.10.012.
24. Penning H, Plugge CM, Galand PE, Conrad R. 2005. Variation of carbon isotope fractionation in hydrogenotrophic methanogenic microbial cultures and environmental samples at different energy status. Global Change Biol 11:2103–2113. https://doi.org/10.1111/j.1365-2486.2005.01076.x.
25. Okumura T, Kawagucci S, Saito Y, Matsui Y, Takai K, Imachi H. 2016. Hydrogen and carbon isotope systematics in hydrogenotrophic methanogenesis under H_2-limited and H_2-enriched conditions: implications for the origin of methane and its isotopic diagnosis. Prog Earth Planet Sci 3:14. https://doi.org/10.1186/s40645-016-0088-3.
26. Schönheit P, Moll J, Thauer RK. 1980. Growth parameters (K_s, μ_{max}, Y_s) of *Methanobacterium thermoautotrophicum*. Arch Microbiol 127:59–65. https://doi.org/10.1007/BF00414356.
27. Morgan RM, Pihl TD, Nölling J, Reeve JN. 1997. Hydrogen regulation of growth, growth yields, and methane gene transcription in *Methanobacterium thermoautotrophicum* ΔH. J Bacteriol 179:889–898. https://doi.org/10.1128/jb.179.3.889-898.1997.
28. Costa KC, Yoon SH, Pan M, Burn JA, Baliga NS, Leigh JA. 2013. Effects of H_2 and formate on growth yield and regulation of methanogenesis in *Methanococcus maripaludis*. J Bacteriol 195:1456–1462. https://doi.org/10.1128/JB.02141-12.
29. Lipson DA. 2015. The complex relationship between microbial growth rate and yield and its implications for ecosystem processes. Front Microbiol 6:615. https://doi.org/10.3389/fmicb.2015.00615.
30. Verhees CH, Kengen SWM, Tuininga JE, Schut GJ, Adams MWW, de Vos WM, van der Oost J. 2003. The unique features of glycolytic pathways in Archaea. Biochem J 375:231–246. https://doi.org/10.1042/bj20021472.
31. Verhaart MRA, Bielen AAM, van der Oost J, Stams AJM, Kengen SWM. 2010. Hydrogen production by hyperthermophilic and extremely thermophilic bacteria and archaea: mechanisms for reductant disposal. Environ Technol 31:993–1003. https://doi.org/10.1080/09593331003710244.
32. Rinker KD, Kelly RM. 1996. Growth physiology of the hyperthermophilic archaeon *Thermococcus litoralis*: development of a sulfur-free defined medium, characterization of an exopolysaccharide, and evidence of biofilm formation. Appl Environ Microbiol 62:4478–4485.
33. Postec A, Pignet P, Cueff-Gauchard V, Schmitt A, Querellou J, Godfroy A. 2005. Optimisation of growth conditions for continuous culture of the hyperthermophilic archaeon *Thermococcus hydrothermalis* and development of sulphur-free defined and minimal media. Res Microbiol 156:82–87. https://doi.org/10.1016/j.resmic.2004.08.001.
34. Morris BEL, Henneberger R, Huber H, Moissl-Eichinger C. 2013. Microbial syntrophy: interaction for the common good. FEMS Microbiol Rev 37:384–406. https://doi.org/10.1111/1574-6976.12019.
35. Weiner A, Schopf S, Wanner G, Probst A, Wirth R. 2012. Positive, neutral and negative interactions in cocultures between *Pyrococcus furiosus* and different methanogenic *Archaea*. Microbiol Insights 5:1–10. https://doi.org/10.4137/MBI.S8516.
36. Lipscomb GL, Schut GJ, Thorgersen MP, Nixon WJ, Kelly RM, Adams MWW. 2014. Engineering hydrogen gas production from formate in a hyperthermophile by heterologous production of an 18-subunit membrane-bound complex. J Biol Chem 289:2873–2879. https://doi.org/10.1074/jbc.M113.530725.
37. Jones WJ, Leigh JA, Mayer F, Woese CR, Wolfe RS. 1983. *Methanococcus jannaschii* sp. nov., an extremely thermophilic methanogen from a submarine hydrothermal vent. Arch Microbiol 136:254–261. https://doi.org/10.1007/BF00425213.
38. Hendrickson EL, Haydock AK, Moore BC, Whitman WB, Leigh JA. 2007. Functionally distinct genes regulated by hydrogen limitation and growth rate in methanogenic Archaea. Proc Natl Acad Sci U S A 104:8930–8934. https://doi.org/10.1073/pnas.0701157104.
39. Mukhopadhyay B, Johnson EF, Wolfe RS. 2000. A novel p_{H2} control on the expression of flagella in the hyperthermophilic strictly hydrogenotrophic methanarchaeon *Methanococcus jannaschii*. Proc Natl Acad Sci U S A 97:11522–11527. https://doi.org/10.1073/pnas.97.21.11522.
40. Enoki M, Shinzato N, Sato H, Nakamura K, Kamagata Y. 2011. Comparative proteomic analysis of *Methanothermobacter thermoautotrophicus* ΔH in pure culture and in coculture with a butyrate-oxidizing bacterium. PLoS One 6:e24309. https://doi.org/10.1371/journal.pone.0024309.
41. Walker CB, Redding-Johanson AM, Baidoo EE, Rajeev L, He Z, Hendrickson EL, Joachimiak MP, Stolyar S, Arkin AP, Leigh JA, Zhou J, Keasling JD, Mukhopadhyay A, Stahl DA. 2012. Functional responses of methanogenic archaea to syntrophic growth. ISME J 6:2045–2055. https://doi.org/10.1038/ismej.2012.60.
42. Luo HW, Zhang H, Suzuki T, Hattori S, Kamagata Y. 2002. Differential expression of methanogenesis genes of *Methanothermobacter thermoautotrophicus* (formerly *Methanobacterium thermoautotrophicum*) in pure culture and in cocultures with fatty acid-oxidizing syntrophs. Appl Environ Microbiol 68:1173–1179. https://doi.org/10.1128/AEM.68.3.1173-1179.2002.
43. Anantharaman V, Koonin EV, Aravind L. 2001. TRAM, a predicted RNA-binding domain, common to tRNA uracil methylation and adenine thiolation enzymes. FEMS Microbiol Lett 197:215–221. https://doi.org/10.1111/j.1574-6968.2001.tb10606.x.
44. Hensley SA, Jung JH, Park CS, Holden JF. 2014. *Thermococcus paralvinellae* sp. nov. and *Thermococcus cleftensis* sp. nov. of hyperthermophilic heterotrophs from deep-sea hydrothermal vents. Int J Syst Evol Microbiol 64:3655–3659. https://doi.org/10.1099/ijs.0.066100-0.
45. Doddema HJ, Vogels GD. 1978. Improved identification of methanogenic bacteria by fluorescence microscopy. Appl Environ Microbiol 36:752–754.
46. Hensley SA, Moreira E, Holden JF. 2016. Hydrogen production and enzyme activities in the hyperthermophile *Thermococcus paralvinellae* grown on maltose, tryptone, and agricultural waste. Front Microbiol 7:167. https://doi.org/10.3389/fmicb.2016.00167.
47. Ver Eecke HC, Akerman NH, Huber JA, Butterfield DA, Holden JF. 2013. Growth kinetics and energetics of a deep-sea hyperthermophilic methanogen under varying environmental conditions. Environ Microbiol Rep 5:665–671. https://doi.org/10.1111/1758-2229.12065.
48. Mook W, Bommerson J, Staverman W. 1974. Carbon isotope fractionation between dissolved bicarbonate and gaseous carbon dioxide. Earth Planet Sci Lett 22:169–176. https://doi.org/10.1016/0012-821X(74)90078-8.
49. Dobin A, Davis CA, Schlesinger F, Drenkow J, Zaleski C, Jha S, Batut P, Chaisson M, Gingeras TR. 2013. STAR: ultrafast universal RNA-seq aligner. Bioinformatics 29:15–21. https://doi.org/10.1093/bioinformatics/bts635.
50. Liao Y, Smyth GK, Shi W. 2014. featureCounts: an efficient general purpose

program for assigning sequence reads to genomic features. Bioinformatics 30:923–930. https://doi.org/10.1093/bioinformatics/btt656.
51. Van Der Maaten L, Hinton G. 2008. Visualizing data using t-SNE. J Mach Learn Res 9:2579–2605.
52. Anders S, Huber W, Nagalakshmi U, Wang Z, Waern K, Shou C. 2010. Differential expression analysis for sequence count data. Genome Biol 11:R106. https://doi.org/10.1186/gb-2010-11-10-r106.
53. Goecks J, Nekrutenko A, Taylor J, Galaxy Team. 2010. Galaxy: a comprehensive approach for supporting accessible, reproducible, and transparent computational research in the life sciences. Genome Biol 11:R86. https://doi.org/10.1186/gb-2010-11-8-r86.
54. Phipson B, Lee S, Majewski IJ, Alexander WS, Smyth GK. 2016. Robust hyperparameter estimation protects against hypervariable genes and improves power to detect differential expression. Ann Appl Stat 10:946–963. https://doi.org/10.1214/16-AOAS920.
55. Kucukural A, Yukselen O, Ozata DM, Moore MJ, Garber M. 2018. DEBrowser: interactive differential expression analysis and visualization tool for count data. bioRxiv https://doi.org/10.1101/399931.